Article

Discovery Medicine 2024; 36(184): 946–958
https://doi.org/10.24976/Discov.Med.202436184.88

Ghrelin Alleviates Inflammation, Insulin Resistance, and Reproductive Abnormalities in Mice with Polycystic Ovary Syndrome via the TLR4-NF-κB Signaling Pathway

Fang Liu[1], Xiaomeng Wang[1], Min Zhao[2], Kexin Zhang[1], Can Li[2], Hong Lin[3], Lin Xu[2,*]

[1]Obstetrics and Gynecology, Qingdao University, 266000 Qingdao, Shandong, China
[2]Department of Obstetrics and Gynecology, Affiliated Hospital of Qingdao University, 266000 Qingdao, Shandong, China
[3]Qingdao Laoshan District Maternal and Child Health Care Family Planning Service Center, 266000 Qingdao, Shandong, China
*Correspondence: xulinqd@qdu.edu.cn (Lin Xu)
Published: 20 May 2024

Background: Polycystic ovary syndrome (PCOS) commonly impacts fertile females with potentially severe effects on fertility and metabolism. Blood ghrelin levels are lower in PCOS patients, and exogenous supplements have been proposed for their potential to trigger anti-inflammatory effects at the cellular level. This study aimed to investigate whether pretreatment with ghrelin reduced inflammation, insulin resistance, and reproductive abnormalities in PCOS and the underlying mechanism of this disorder.

Methods: Ghrelin supplementation was first tested in an inflammation model using human ovarian granulosa cells (KGN cells) that were built by treated with Lipolyaccharide. KGN cells were pretreated with ghrelin and exposed to lipopolysaccharide (LPS). Inflammatory gene expression and cytokine production were analyzed by Enzyme-linked immunosorbent assay (ELISA). Based on these results, the PCOS mice model was built with Dehydroepiandrosterone (DHEA) and a high-fat diet. The mRNA and protein expressions of inflammatory factors including Toll-like receptor 4 (TLR4), nuclear factor kappa-B-p65 (NF-κB-p65), Phospho-NF-κB-p65 (p-NF-κB-p65) and myeloid differentiation factor 88 (MYD88) related to the TLR4/NF-κB signaling pathway were evaluated in KGN cells and mouse ovarian tissues using Real-Time Quantitative Polymerase Chain Reaction (RT-qPCR) and western blot, respectively. Lipid metabolism was quantified via an automated biochemical analyzer.

Results: The mRNA and protein expressions of interleukin-6 (IL-6), interleukin-1 beta (IL-1β), and tumor necrosis factor alpha (TNF-α) in ghrelin pretreated KGN cells were lower than the LPS group ($p < 0.05$). Protein expression was reduced for TLR4, NF-κB-p65, and MYD88 within KGN cells of ghrelin groups compared to the LPS group ($p < 0.05$). Ghrelin treatment restored the estrous cycle and slowed weight gain and abdominal fat weight of PCOS mice ($p < 0.05$). Ghrelin treatment decreased the serum concentrations of testosterone, luteinizing hormone, insulin, IL-6, IL-1β, and TNF-α compared to the PCOS group ($p < 0.05$). Estradiol concentrations of mice treated with ghrelin were higher than the PCOS group ($p < 0.05$). The concentrations of low and high-density lipoprotein, triglyceride, and cholesterol in mice treated with ghrelin were lower than in the PCOS mice ($p < 0.05$). Inflammatory gene expression for IL-6, IL-1β, TNF-α, TLR4, NF-κB-p65, and MYD88 decreased in the ovarian tissues of ghrelin-treated mice compared to the PCOS group ($p < 0.05$), along with reduced protein expression of TLR4, p-NF-κB-p65, and MYD88 ($p < 0.05$).

Conclusions: In the present study, ghrelin treatment effectively reduced inflammation *in vitro*, and attenuated insulin resistance and reproductive abnormalities in PCOS mice through the TLR4/NF-κB signaling pathway, highlighting potential therapeutic avenues for future PCOS treatments and research directions.

Keywords: ghrelin; polycystic ovary syndrome; inflammation; insulin resistance; lipid metabolism

Introduction

The primary cause of infertility resulting from ovulation abnormalities is often attributed to polycystic ovary syndrome (PCOS), a condition characterized by polycystic ovary modification, oligovulation or anovulation, and hyperandrogenemia [1,2]. This condition may potentially lead to several clinical manifestations, including menstrual abnormalities, infertility, acne, and hirsutism. Nevertheless, the precise pathophysiological mechanisms behind PCOS have yet to be fully elucidated. Genetic differences have been identified as a contributing factor to the pathophysiology of PCOS in many investigations [3,4]. Furthermore, it has been shown that there is a correlation between insulin resistance and the pathophysiology of PCOS [5,6]. How chronic low-level inflammation might be involved in PCOS pathogenesis has been the subject of scientific inquiry [7,8].

The mRNA expression for the inflammatory mediators such as tumor necrosis factor alpha (TNF-α), interleukin-6 (IL-6), and interleukin-1 beta (IL-1β) increased in the ovarian granulosa cells of PCOS patients compared to women without the condition [9]. Furthermore, previous studies have observed elevated IL-1β and IL-6 levels in the serum of PCOS subjects compared to the general population [10–12]. In contrast, previous research has shown that the reduction of PCOS-related symptoms is accompanied by a corresponding decrease in levels of inflammatory-related variables [13,14]. These studies suggest inflammation might be involved in the development of PCOS.

Ghrelin is a growth hormone-releasing peptide primarily produced by P/D1 cells in the stomach and vital for regulating insulin sensitivity, satiety, and energy levels [15]. Previous research has shown that PCOS subjects have reduced levels of ghrelin in their blood serum as compared to those without the condition [16,17]. A further investigation provided evidence suggesting that ghrelin may potentially enhance pancreatic insulin production in overweight individuals [18]. Moreover, it was shown that ghrelin may mitigate inflammatory gastritis and lung injury in rats [19,20]. However, there are no studies showing whether ghrelin can affect PCOS.

Therefore, we hypothesized that ghrelin might have a similar impact on PCOS and conducted this investigation to study its mechanism.

Methods and Materials

Cell Lines

The KGN cell lines, verified by STR identification and mycoplasma detection, were acquired from Procell (CL-0603, Wuhan, China) and maintained in Dulbecco's Modified Eagle Medium (DMEM)/F12, supplemented with 10% fetal bovine serum and 1% solution of penicillin-streptomycin (PM150312, PM180120, Procell, Wuhan, China). The cells were cultivated at 5% concentration of CO_2 and 37 °C.

Grouping and Treatment

As described in previous studies [21–24], KGN cells were subjected to a 24-hour exposure to lipopolysaccharide (LPS, T11855, Target Molecule Corp., Shanghai, China) at 1 µg/mL to elicit an inflammatory response. The cells underwent an overnight incubation and were divided into six distinct groups: the control, the LPS, the LPS + 100 ng/mL ghrelin, the LPS + 200 ng/mL ghrelin, the LPS + 300 ng/mL ghrelin, and the LPS + 400 ng/mL ghrelin groups (S23009, Yuanye Biotechnology Co., Ltd., Shanghai, China). The KGN cells in the control and the LPS groups were grown in DMEM/F12 medium for 24 hours. They were subjected to several doses (100, 200, 300, and 400 ng/mL) of human ghrelin in DMEM/F12 medium for 24 hours. In the control group, DMEM/F12 alone was subsequently used. On the other hand, cells belonging to the remaining groups were subjected to LPS (1 µg/mL) in DMEM/F12 for 24 hours. To explore the role of the Toll-like receptor 4 (TLR4)/nuclear factor kappa-B (NF-κB) signaling pathway, the cells were pretreated with 5 µM TAK242 (HY-11109, MedChemExpress, Shanghai, China), a selective inhibitor of TLR4 signaling, for 24 hours before being exposed to LPS to block the TLR4 pathway.

Animals

A total of twenty-four female, 21-day old, 15.63 $\pm$ 0.87 g mice (C57BL/6J) could be procured via Jinan Pengyue Experimental Animal Breeding Co., Ltd. (Certificate No. SCXK [Lu] 2022 0006 Shandong, China). The animals were housed at 24 °C and maintained in 12-hour light-dark cycles daily. Tap water and food supply were not restricted and were continuously provided. The experiment underwent a thorough evaluation and received approval from the Animal Ethics Review Committee of the Affiliated Hospital of Qingdao University. It was carried out in strict adherence to the standards set out by the committee.

Experimental Animal Model of PCOS

The flow chart of the animal experiment is shown in Fig. 1. Following one week of adaptive feeding, the mice were allocated into three groups (n = 8) via a randomization process. The control group was provided with a standard control diet for six weeks and received a subcutaneous injection of 100 µL of maize oil daily for three weeks. The PCOS and ghrelin treatment groups were provided with a high-fat diet (XTHF60, Jiangsu Xietong Pharmaceutical Bioengineering Co., Ltd., Jiangsu, China) containing 60% fat energy for six weeks. Additionally, a daily Dehydroepiandrosterone (DHEA, 60 mg/kg body weight, GC11070, GLPBIO, Shanghai, China) diluted within 100 µL of corn oil was subcutaneously injected for three weeks. Following a treatment period of three weeks, including DHEA administration, the control and PCOS groups were subjected to daily gavage with 100 µL saline. The experimental group received a daily intragastric administration of 100 µL of ghrelin (0.8 mg/kg body weight, Y32519, Yuanye Biotechnology Co., Ltd., Shanghai, China) diluted within 100 µL of saline solution as described in a previous study [25]. During the experiment, the mice were weighed weekly, and Lee's index calculation was performed as body weight $(g)^{\wedge 1/3} \times 10$/body length (cm). At the end of the experiment, the mice were euthanized using CO_2. Blood, bilateral ovarian tissue, and visceral adipose tissue were collected and kept within –80 °C for subsequent experiments.

Estrous Cycle Determination

Vaginal smears were used throughout the third and sixth weeks of the study to ascertain the estrous cycle on a daily basis at 9:00 a.m.

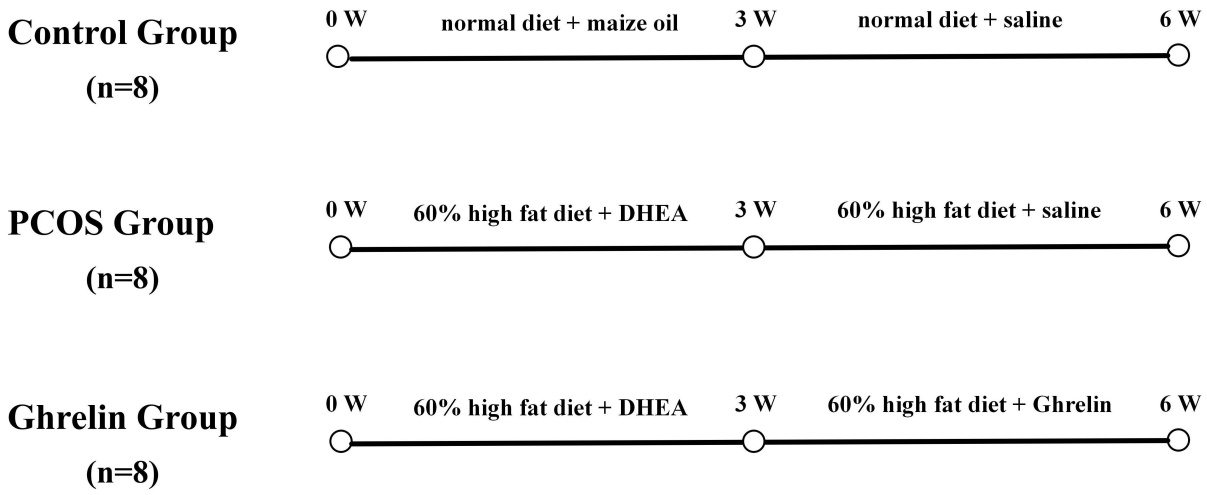

Fig. 1. Flow chart of animal experiment. PCOS, polycystic ovary syndrome; W, week.

Intraperitoneal Insulin and Glucose Tolerance Tests

Three days before the experiment ended, the mice within each group were randomly divided into two separate groups. This division was carried out specifically for conducting intraperitoneal glucose and insulin tolerance tests (IPGTT and ITT). The blood samples were collected from the tail of the mice. Following the assessment of fasting glucose levels, the mice designated for the ITT received intraperitoneal injections of D-glucose (g8270, Sigma–Aldrich, Saint Louis, MO, USA, 2 g/kg body weight as a 50% glucose stock), whereas the animals assigned to the IPGTT were administered insulin (1 IU/kg body weight, Humalog Mix25, China) by intraperitoneal injection. Blood glucose levels were assessed at 15, 30, 60, 90, and 120 minutes. The formula homeostasis model assessment-insulin resistance (HOMA-IR) = FBG (mmol/L) $\times$ FINS (mU/L)/22.5 computed the HOMA-IR index.

Lipid Metabolism

Low- and high-density lipoprotein (LDL and HDL), triglyceride (TG), and cholesterol (CHO) concentrations in the blood from the mice were quantified via an automated biochemical analyzer (Chemray 800, Chemray, Shenzhen, China).

Hematoxylin-Eosin (HE) Staining

A 4% paraformaldehyde solution-based fixation of remaining adipose tissues and ovaries was performed at 25 °C for 24 hours. Following paraffin embedding and tissue dehydration, adipose and ovarial sectioning was conducted via a tissue slicer into serial sections (5 µm each). The sections underwent staining using commercially available hematoxylin and eosin kits (C0105, Beyotime, Shanghai, China). Then, the ovarian sections were viewed using a panoramic biopsy scanner (PANNORAMIC DESK/MIDI/250/1000, 3DHISTECH (Budapest, Hungary)). The adipose sections were viewed using an upright white light photographic microscope (Nikon, Tokyo, Japan) and analyzed using Image-Pro Plus 6.0 (Media Cybemetics, Rockville, MD, USA).

Enzyme-Linked Immunosorbent Assay (ELISA)

TNF-α (E-EL-H0109, Elabscience, Wuhan, China), IL-6 (E-EL-H6156, Elabscience, Wuhan, China), and IL-1β (E-EL-H0149, Elabscience, Wuhan, China) amounts within the supernatants were determined using ELISA kits. Additionally, luteinizing hormone (LH, CEA441Mu, Wuhan USCN Business Co., Ltd., Wuhan, China), insulin (INS, CEA448Mu, Wuhan USCN Business Co., Ltd., Wuhan, China), IL-6 (GEM0001, Servicebio, Wuhan, China), IL-1β (GEM0002, Servicebio, Wuhan, China), TNF-α (GEM0004, Servicebio, Wuhan, China) follicle-stimulating hormone (FSH, CEA830Mu, Wuhan USCN Business Co., Ltd., Wuhan, China), estrogen (E_2, CEA461Ge, Wuhan USCN Business Co., Ltd., Wuhan, China), and testosterone (T, GEM0014, Servicebio, Wuhan, China) serum concentrations were measured using ELISA kits, following the procedure provided by the manufacturer.

Real-Time Quantitative Polymerase Chain Reaction (RT-qPCR) and RNA Isolation

RNA extraction and isolation were performed with FreeZol Reagent (R711, Vazyme, Nanjing, China) to extract RNA from the whole sample. After measuring the concentration and purity of RNA using a Qubit fluorometer (840-317400, ThermoFisher Scientific, Waltham, MA, USA), we employed 1–2 µg of total RNA to generate synthetic cDNA via an All-In-One 5X RT MasterMix Kit (G592, Abm, Zhenjiang, China). The measurement of mRNA expression levels was conducted using the Blas-

Table 1. RT-qPCR primers of KGN cells.

Genes	Primers	Sequence 5′-3′
GAPDH	Forward	GCACCGTCAAGGCTGAGAAC
	Reverse	TGGTGAAGACGCCAGTGGA
TNF-α	Forward	TGCACTTTGGAGTGATCGGC
	Reverse	GCTTGAGGGTTTGCTACAACA
IL-6	Forward	AGAGGCACTGGCAGAAAACA
	Reverse	TCACCAGGCAAGTCTCCTCA
IL-1β	Forward	AACCTCTTCGAGGCACAAGG
	Reverse	GTCCTGGAAGGAGCACTTCAT

RT-qPCR, Real-Time Quantitative Polymerase Chain Reaction; *GAPDH*, glyceraldehyde-3-phosphate dehydrogenase; TNF-α, tumor necrosis factor alpha; *IL-6*, interleukin-6; *IL-1β*, interleukin-1 beta.

Table 2. RT-qPCR primers of ovarian tissue.

Genes	Primers	Sequence 5′-3′
NF-κB	Forward	CTCTGGCACAGAAGTTGGGT
	Reverse	TCCCGGAGTTCATCTCATAGT
TLR4	Forward	TCCCTGCATAGAGGTAGTTCC
	Reverse	TCAAGGGGTTGAAGCTCAGA
TNF-α	Forward	ACCCTCACACTCACAAACCA
	Reverse	ATAGCAAATCGGCTGACGGT
IL-1β	Forward	TGCCACCTTTTGACAGTGATG
	Reverse	AAGGTCCACGGGAAAGACAC
IL-6	Forward	TTCCATCCAGTTGCCTTCTTGG
	Reverse	ACAGGTCTGTTGGGAGTGGTATC
MYD88	Forward	GCATATGCCTGAGCGTTTCG
	Reverse	ATCCGGCGGCACCCAC
β-actin	Forward	CCACTGTCGAGTCGCGTC
	Reverse	ATTCCCACCATCACACCCTGG

NF-κB, nuclear factor kappa-B; *TLR4,* Toll-like receptor 4; *MYD88*, myeloid differentiation factor 88.

Taq™ 2X qPCR MasterMix kit (G891, Abm, Zhenjiang, China). The $2^{-\Delta\Delta Ct}$ technique was utilized for determining relative gene expression. Tables 1,2 exhibit the primers.

Western Blotting

The proteins were solubilized in a sodium dodecyl sulfate lysis solution with 10% phosphatase and protease inhibitors obtained from Solarbio (P1260, Beijing, China). Following the determination of protein concentration (ZJ102, EpiZyme, Shanghai, China), protein separation was carried out using electrophoresis on a dodecyl sulfate-polyacrylamide gel. Polyvinylidene fluoride membranes (Millipore, Burlington, MA, USA) were employed for protein blotting, with a duration of 1 to 1.5 hours and an electrical current of 290 mA. This duration and current were chosen to facilitate the binding of proteins to the membrane. The membranes were blocked with a 5% non-fat milk solution in phosphate-buffered solution-Tween-20 for one hour at 25 °C. Following this, an overnight incubation was conducted at 4 °C with the following primary antibodies: myeloid differentiation factor 88 (MYD88) (1:8000 dilution, 67969-1-Ig, Proteintech, Rosemont, IL, USA), α-Tubulin (1:50,000 dilution, 66031-1-Ig, Proteintech, Rosemont, IL, USA), phospho-NF-κB p65 (p-NF-κB-p65) (1:1000 dilution, 3033, Cell Signaling Technology, Danvers, MA, USA), NF-κB p65 (1:4000 dilution, 80979-1-RR, Proteintech, Rosemont, IL, USA), TLR4 (1:4000 dilution, 66350-1-Ig, Proteintech, Rosemont, IL, USA), and GAPDH (1:5000 dilution, E-AB-40337, Elabscience, Wuhan, China). Then, the secondary antibodies (diluted at 1:5000, E-AB-1001, E-AB-1003, Elabscience, Wuhan, China) were applied to the membranes at room temperature, subsequent to being conjugated with horseradish peroxidase for one hour. The chemiluminescence technique was employed for detecting the signals (GGNOME-XRQ-NPC, GeneGnome, Hongkong, China), and the gray value was measured using Image J software (National Institutes of Health, Bethesda, MD, USA).

Data Analysis

GraphPad Prism (version 9.0, GraphPad Software, Inc., San Diego, CA, USA) executed all analytical processes. *T*-tests were used for statistical analysis to compare experiments involving two groups. A one-way analysis of variance followed by Tukey's multiple comparisons test was used for experiments containing more than two groups. Data presented as mean ± standard deviation (SD). The threshold of $p < 0.05$ was considered statistically significant.

Results

Ghrelin Attenuated the mRNA Expression of LPS-induced Inflammation-Related Factors in KGN Cells

The inflammatory response of KGN cells was assessed via RT-qPCR after LPS treatment. As shown in Fig. 2A–C, IL-6, IL-1β, and TNF-α mRNA expression exhibited significant elevations among LPS-treated cells compared to the control cells ($p < 0.05$). IL-6, IL-1β, and TNF-α expression values of mRNA were significantly diminished after pretreatment with ghrelin compared to the cells treated with LPS ($p < 0.05$). As shown in Fig. 2D–F, the administration of TAK242 effectively suppressed IL-6, IL-1β, and TNF-α mRNA upregulation produced via LPS among KGN cells. Moreover, IL-6 mRNA expression was dropped after pretreatment with 100 and 200 ng/mL ghrelin ($p < 0.05$). The mRNA expression of IL-1β was also decreased after pretreatment with 100 ng/mL ghrelin ($p < 0.05$). The IL-6, IL-1β, and TNF-α mRNA expressions of other ghrelin groups were lower than the TAK242 group; however, there was no statistical difference ($p > 0.05$).

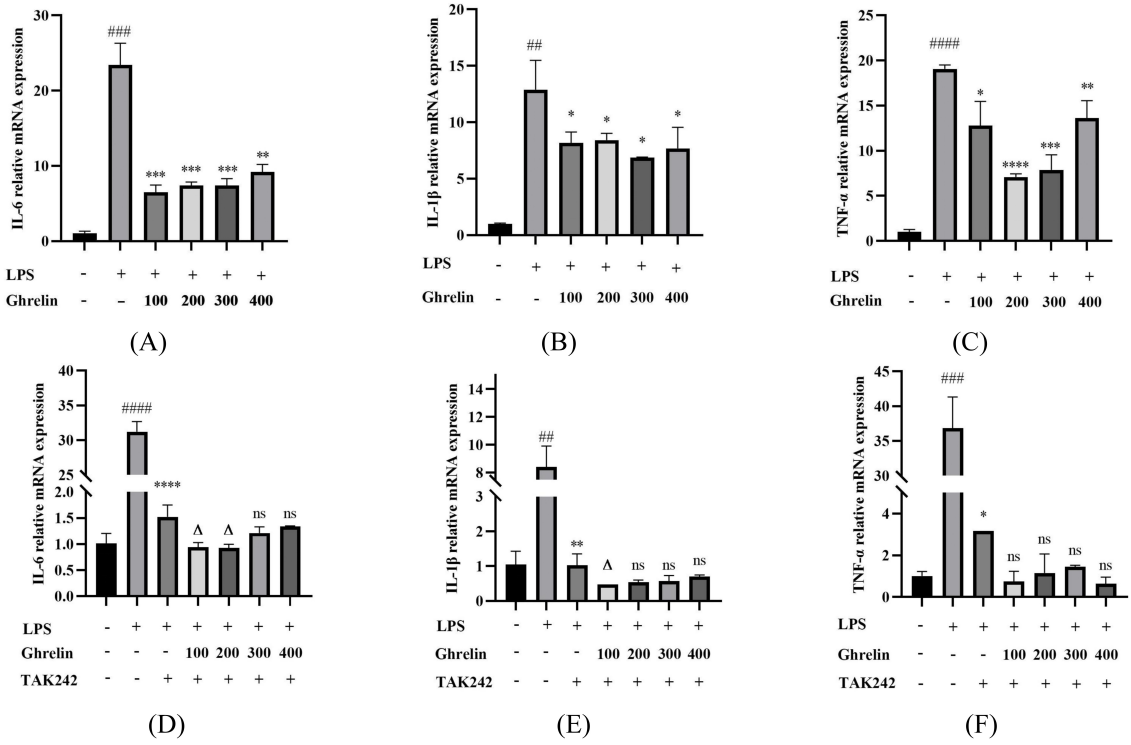

Fig. 2. Ghrelin attenuated IL-6, IL-1β, and TNF-α mRNA expression of KGN cells based on RT-qPCR (n = 3). (A–C) 1 µg/mL lipopolysaccharide (LPS) treatment for 24 h was employed following different ghrelin measurements (0, 100, 200, 300, or 400 ng/mL) could be utilized for treating KGN cells for 24 h. (D–F) The previous intervention with TAK242 and similar ghrelin concentrations, was followed by a similar LPS administration regimen. $^{\#\#}$, $^{\#\#\#}$ and $^{\#\#\#\#}$: $p < 0.01$, 0.001 and 0.0001 vs. control group; *, **, *** and ****: $p < 0.05$, 0.01, 0.001 and 0.0001 vs. LPS group; $^{\Delta}$: $p < 0.05$ vs. LPS+TAK242 group; ns: no statistical difference vs. LPS+TAK242 group. IL-6, interleukin-6; IL-1β, interleukin-1 beta; TNF-α, tumor necrosis factor alpha.

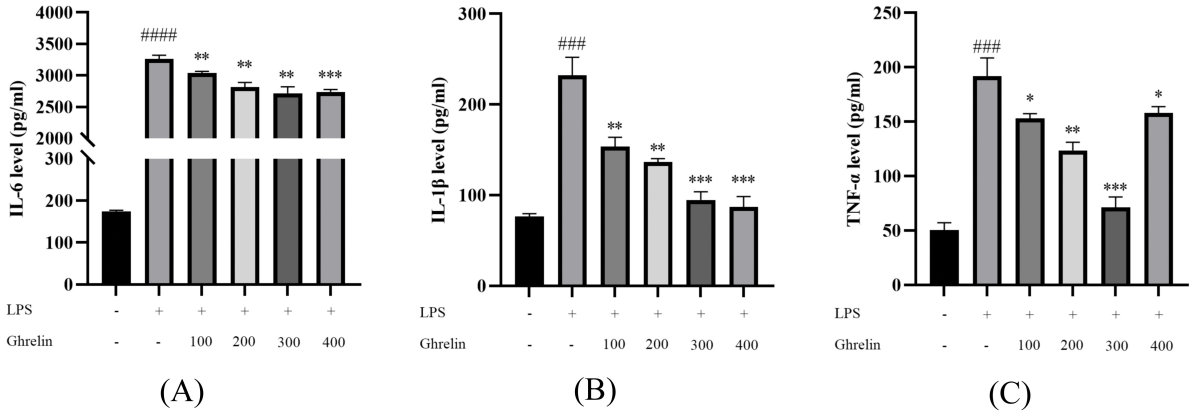

Fig. 3. Ghrelin attenuated IL-6, IL-1β, and TNF-α expression of KGN cells based on ELISA (n = 3). The amount of (A) IL-6, (B) IL-1β, and (C) TNF-α detected in the supernatant of KGN cells pretreated with 24 h ghrelin (0, 100, 200, 300, or 400 ng/mL) and exposed to LPS for 24 h (1 µg/mL). $^{\#\#\#}$ and $^{\#\#\#\#}$: $p < 0.001$ and 0.0001 vs. control group; *, ** and ***: $p < 0.05$, 0.01 and 0.001 vs. LPS group. ELISA, Enzyme-linked immunosorbent assay.

Ghrelin Attenuated the Protein Levels of LPS-Induced Inflammation-Related Factors in KGN Cells

The presence of inflammatory cytokines in KGN cells was assessed via ELISA. As shown in Fig. 3A–C, IL-6, IL-1β, and TNF-α protein levels were significantly elevated among LPS-treated cells than in control cells ($p < 0.05$). The ghrelin-treated groups had reduced IL-6, TNF-α, and IL-1β protein values than LPS-treated cells ($p < 0.05$).

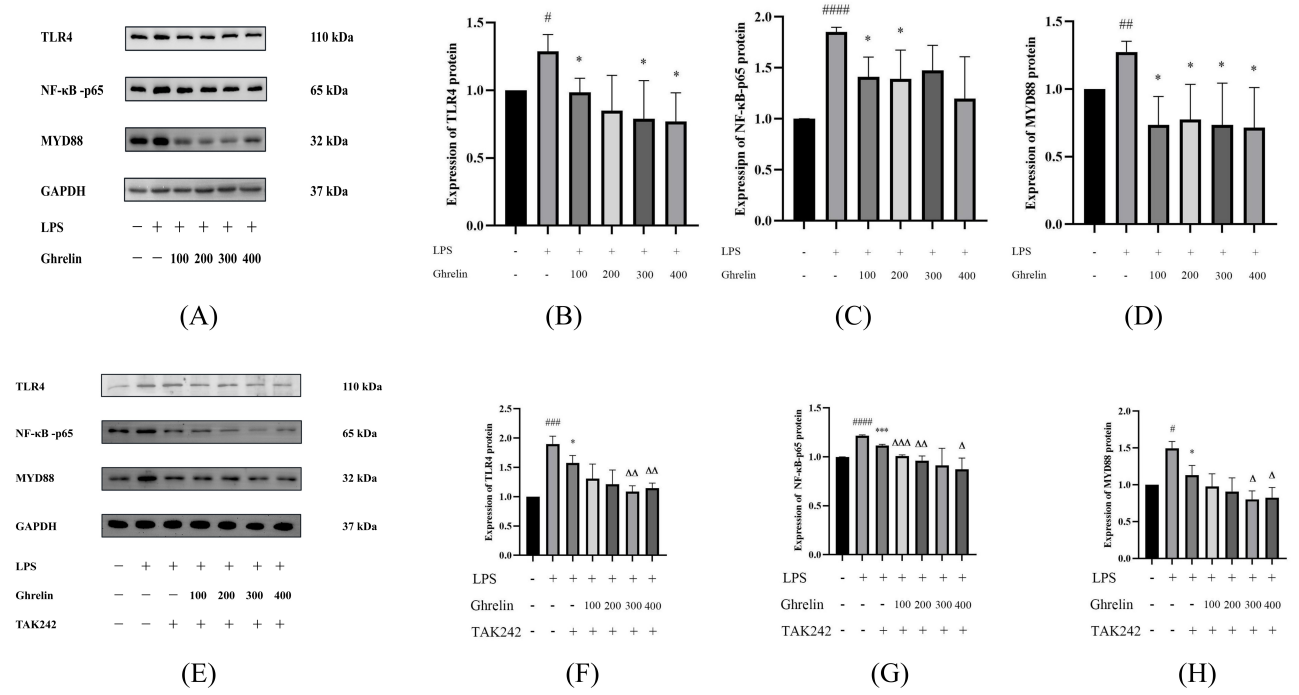

Fig. 4. Western blotting-based KGN cell-related NF-κB-p65, TLR4, and MYD88 protein expression (n = 3). (A–D) 1 µg/mL LPS treatment employed following different ghrelin measurements (0, 100, 200, 300, or 400 ng/mL) for 24 h could be utilized for treating KGN cells for 24 h. (E–H) The previous intervention with TAK242 and similar ghrelin concentrations was followed by a similar LPS regimen. $^{\#}$, $^{\#\#}$, $^{\#\#\#}$ and $^{\#\#\#\#}$: $p < 0.05$, 0.01, 0.001, and 0.0001 vs. control group; * and ***: $p < 0.05$ and 0.001 vs. LPS group; $^{\Delta}$, $^{\Delta\Delta}$ and $^{\Delta\Delta\Delta}$ vs. LPS+TAK242 group. MYD88, myeloid differentiation factor 88.

Ghrelin Affected TLR4, NF-κB p65, and MYD88 Protein Expressions

Western blotting was used to assess the LPS-mediated MYD88, TLR4, and NF-κB p65 expression among KGN cells. MYD88, TLR4, and NF-κB p65 expression among KGN cells was elevated by LPS ($p < 0.05$), as shown in Fig. 4A–D. Nevertheless, ghrelin administration before the LPS exposure significantly mitigated this impact ($p < 0.05$). However, the administration of TAK242 resulted in substantial suppression of both TLR4, NF-κB p65, and MYD88 expression, and ghrelin administration led to further reductions in MYD88 and NF-κB p65 levels ($p < 0.05$), as shown in Fig. 4E–H.

PCOS Model Confirmation

As described in previous studies, PCOS mice are characterized by disturbance of the estrous cycle and insulin resistance [26,27]. A vaginal smear test was conducted to monitor the estrous cycle during the experimental period to assess the formation of the PCOS model. The control group exhibited normal estrus, but the PCOS group had a predominance of mice in the metestrus and diestrus stages (Fig. 5A), which is a characteristic pathological manifestation of PCOS. As shown in Fig. 5B–D, blood glucose and insulin levels exhibited a statistically significant increase in mice with PCOS ($p < 0.05$). The HOMA-IR index exhibited a remarkable rise in mice with PCOS ($p < 0.05$), suggesting that the PCOS model was effectively produced.

Ghrelin Slowed Weight Gain

The mice underwent weekly weighing (Fig. 6A). At the start of the trial, there was an absence of mice body weight disparity. Within the experimental six weeks, a notable rise in body weight could be seen in the mice with PCOS compared to the controls. As shown in Fig. 6B, in contrast to the PCOS group, the ghrelin exhibited a propensity for body weight reduction ($p < 0.05$). The mice in the PCOS group had a greater nasoanal length than the mice control and the ghrelin groups ($p < 0.05$), as shown in Fig. 6C. No discernible differences were seen among the control, PCOS, and ghrelin groups ($p > 0.05$), as shown in Fig. 6D.

Ghrelin Improved the Ovarian Function of PCOS Mice

The cycle phases of the mice in each group were conducted daily throughout the last week of the experiment. It was observed that the mice belonging to the control and ghrelin groups mostly exhibited a consistent estrous cycle, whereas those in the PCOS one consistently remained in the diestrus condition (Fig. 7A). Ovarian pathological alternations were examined via HE staining (Fig. 7B). Compared

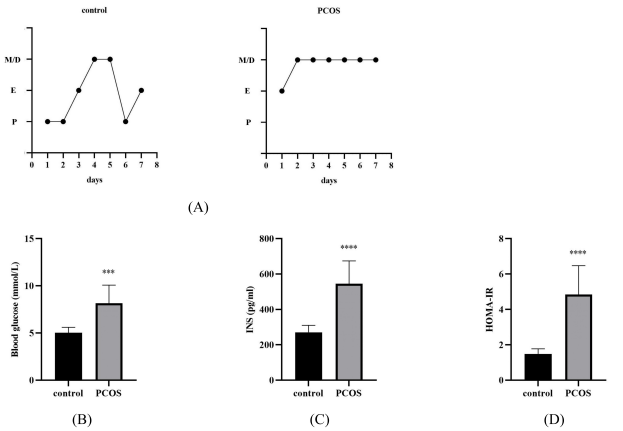

Fig. 5. PCOS mouse model establishment (Control group: n = 8; PCOS group: n = 16). (A) The mice's estrous cycle was observed via the vaginal smear approach. M, Metestrus; D, Diestrus; P, Proestrus; E, Estrus. Each group's estrous cycle on the third week for seven consecutive days. (B) After fasting overnight, the glucose oxidase approach was employed to measure the mice's blood glucose. (C) ELISA-based mice serum insulin levels after fasting overnight. (D) Following serum mice insulin and glucose levels, HOMA-IR was estimated. *** and ****: $p < 0.001$ and 0.0001 vs. control group. PCOS, polycystic ovary syndrome; IR, insulin resistance.

with the control group, the PCOS group had more cystic and immature follicles. However, the number of cystic and immature follicles in the ghrelin group was less than that in the PCOS group. The data shown in Fig. 7C demonstrates a considerable decrease in the number of corpora lutea in mice with PCOS ($p < 0.05$). In contrast, the ghrelin group had a progressive augmentation in the quantity of corpora lutea ($p < 0.05$).

Ghrelin Enhanced PCOS Mice Abdominal Fat Weight and Size of Adipocytes

Fig. 8A–C demonstrates that the application of HE staining revealed an increase in both the diameter and area of adipocytes in the PCOS group compared to controls ($p < 0.05$). Nevertheless, administration of ghrelin effectively counteracted this observed trend ($p < 0.05$). Fig. 8D indicates a remarkable rise in abdominal fat within the PCOS group compared to the control and ghrelin groups ($p < 0.05$).

Ghrelin Regulated PCOS by Improving Sex Hormone Levels

To assess the effects of ghrelin in mitigating PCOS, quantities of E_2, T, LH, and FSH were quantified in each experimental group of mice via ELISA (Fig. 9). In contrast to controls, PCOS-treated cells had a drop in E_2 concentration and increased T and LH concentrations ($p < 0.05$). There was no remarkable difference in FSH concentration between the controls and the group with PCOS ($p > 0.05$). Nevertheless, the LH/FSH ratio in the PCOS group exhibited a remarkable increase compared to the controls ($p < 0.05$). Compared with the PCOS mice, the mice treated with ghrelin had a higher concentration of E_2 and a lower concentration of T ($p < 0.05$). No discernible disparity was seen in the LH and FSH levels between the groups administered with ghrelin and PCOS group ($p > 0.05$). The ratio of LH to FSH was remarkably more diminished within the ghrelin-treated than in the PCOS group ($p < 0.05$).

Ghrelin Reduced Insulin Resistance in PCOS Mice

The insulin concentration in mice blood was quantified by ELISA. This measurement aimed to examine the insulin resistance (IR) index within the PCOS model and investigate ghrelin's impact on IR (Fig. 10). In contrast to the control group, the PCOS mice exhibited remarkably elevated levels of insulin content and HOMA-IR indices ($p < 0.05$). However, administration of ghrelin effectively mitigated this observed trend ($p < 0.05$). The findings of this study suggest that ghrelin might mitigate IR related to PCOS. Then, we used GraphPad Prism software to calculate the area under the curve (AUC) of ITT and IPGTT-related FBG. The results show an increase in the PCOS group compared with the control group ($p < 0.05$). However, after treatment with ghrelin, these parameters exhibited a significant reduction ($p < 0.05$).

Ghrelin Improved Lipid Metabolism in PCOS Mice

An automated biochemical analyzer was employed to identify four serum lipid biochemical markers in mice to further validate alterations in blood lipid levels. As shown in Fig. 11A–D, TG, CHO, LDL-C, and HDL-C levels were elevated in the PCOS compared to controls ($p < 0.05$). Ghrelin-treated TG, LDL-C, and HDL-C concentrations were lower than the PCOS group ($p < 0.05$). CHO concentrations were not significantly different ($p > 0.05$).

Ghrelin Alleviated Inflammation in PCOS Mice

To assess the impact of ghrelin on ovarian inflammation, RT-qPCR was used to measure the inflammation markers-related mRNA expression values in ovarian tissue. The results are shown in Fig. 12A–C. IL-6, IL-1β, and TNF-α mRNA expression values were considerably elevated among PCOS cells than controls ($p < 0.05$) and were remarkably reduced in the mice treated with ghrelin, as compared to those in the PCOS group ($p < 0.05$).

Moreover, ELISA kits were utilized to quantify alterations in these markers within the serum of mice, aiming to investigate the potential association between PCOS and markers associated with an inflammatory environment (Fig. 12D–F). IL-6, IL-1β, and TNF-α concentrations were elevated with PCOS ($p < 0.05$) compared to controls. However, after treatment with ghrelin, these concentrations exhibited a significant reduction ($p < 0.05$).

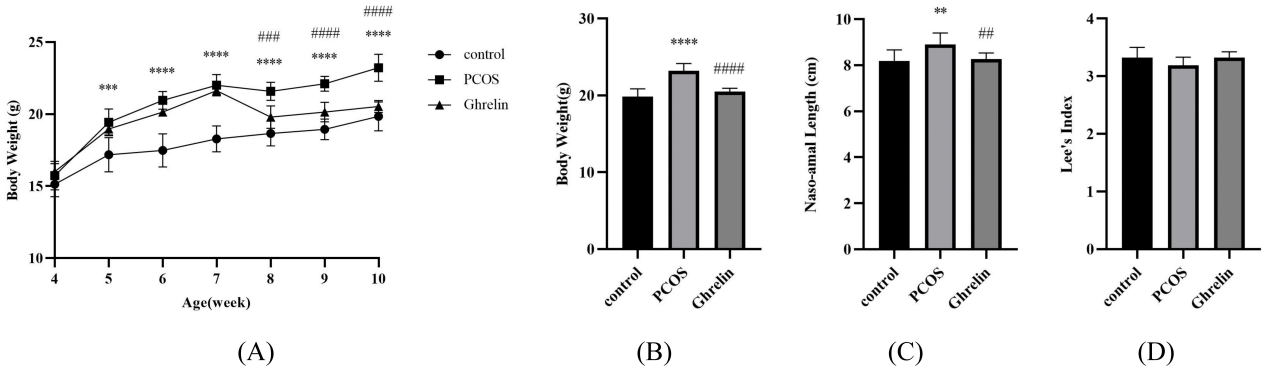

Fig. 6. Ghrelin impact on body weight and nasoanal length (n = 8). (A) The pattern of body weight fluctuations in the mice during six consecutive weeks within each experimental group. The diagrams of (B) body weight difference diagram, (C) nasoanal length, and (D) Lee's index are all in the sixth week for the three groups. **, *** and ****: $p < 0.01$, 0.001 and 0.0001 vs. control group; similarly, ##, ###, and ####: $p < 0.01$, 0.001 and 0.0001 vs. PCOS group.

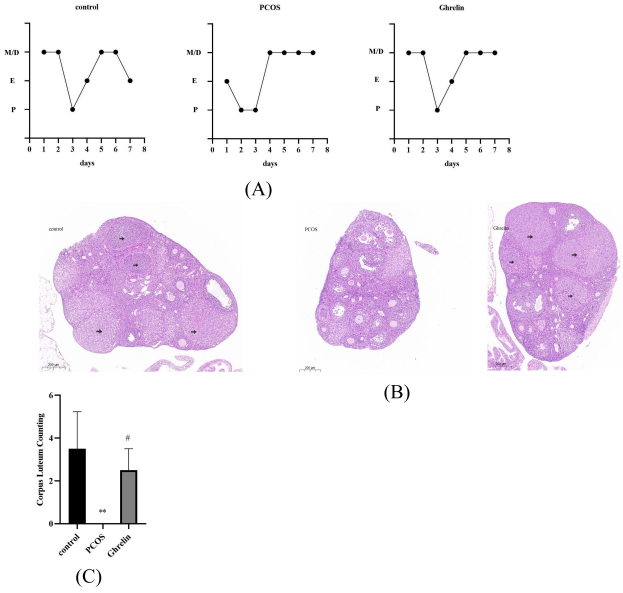

Fig. 7. Ghrelin regulated the PCOS-related estrous cycle disorder and improved ovarian pathological characteristics. (A) Mice estrous cycle within the three groups on the sixth week for seven consecutive days. (B) HE-stained mouse ovaries of the mice in the three groups (scale bar: 200 µm, the arrow indicates corpus luteum). (C) The corpus luteum counts of the mice in the three groups (n = 8). **: $p < 0.01$ vs. control group; #: $p < 0.05$ vs. PCOS group. HE, Hematoxylin-eosin.

Ghrelin Might Ameliorate Mice PCOS through the Signaling Pathway TLR4/NF-κB

Within mice ovarian tissues, RT-qPCR was employed for assessing TLR4, NF-κB, and MYD88 genetic expression values associated with the TLR4 signaling pathway. As shown in Fig. 13A–C, the mRNA expression of TLR4, NF-κB, and MYD88 was not different among the PCOS and control groups ($p > 0.05$). However, the treated group exhibited lower expression levels than the PCOS group ($p < 0.05$).

Moreover, western blotting was utilized for semi-quantifying MYD88, p-NF-κB-p65, NF-κB-p65, and TLR4 protein expression in ovarian tissues. This was done to provide further confirmation about the protein alterations related to the TLR4/NF-κB pathway. As shown in Fig. 13D–H, compared with controls, PCOS-treated mice exhibited more elevated MYD88, TLR4, and p-NF-κB-p65 expression ($p < 0.05$). Moreover, the expression of MYD88, TLR4, and p-NF-κB-p65 protein was lower with ghrelin ($p < 0.05$). However, there was no significant alteration in NF-κB-p65 expression ($p > 0.05$).

Discussion

PCOS is a prevalent gynecological disorder that affects women throughout their adolescence and reproductive years. This condition significantly impacts individuals' emotional and physical well-being, leading to a substantial burden [28–30]. Hence, identifying a pharmaceutical compound that exhibits exceptional therapeutic effectiveness and limited adverse reactions has considerable importance.

Ghrelin is an endogenous peptide consisting of 28 amino acids, which can induce growth hormone secretion. Furthermore, ghrelin has a role in several neuroendocrine mechanisms, such as the synthesis of prolactin and adrenocorticotropin [31]. Previous studies have shown that ghrelin elicits several effects, such as hypotension, suppression of inflammation, and increased apoptosis [32–34]. In a study conducted by Ge *et al.* [35], it was shown that the administration of ghrelin prior to treatment enhanced the beneficial effects of conditioned media produced from bone marrow-derived mesenchymal stem cells in mitigating the detrimen-

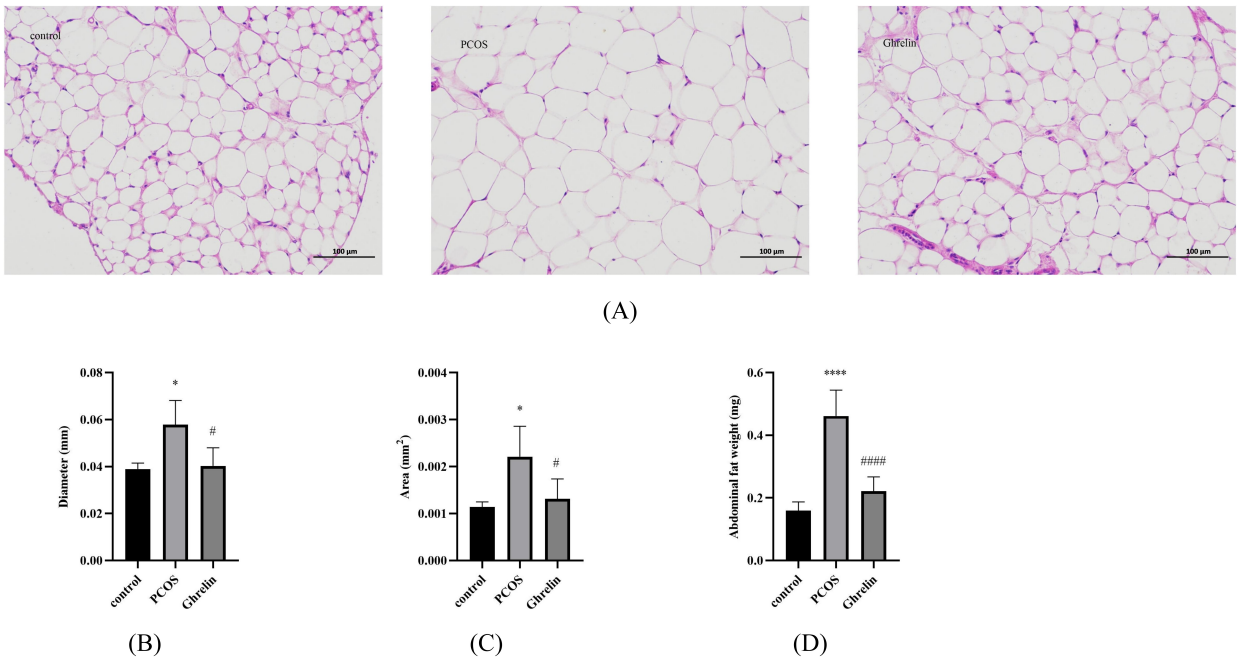

Fig. 8. Abdominal fat weight and adipocyte size improvements via ghrelin in PCOS mice (n = 8). (A) Mice adipose tissue HE sections (scale bar: 100 μm). (B) Area of adipocyte in abdominal adipose tissue. (C) Diameter of adipocyte in abdominal adipose tissue. (D) Abdominal fat weight. * and ****: $p < 0.05$ and 0.0001 vs. control group; # and ####: $p < 0.05$ and 0.0001 vs. PCOS group.

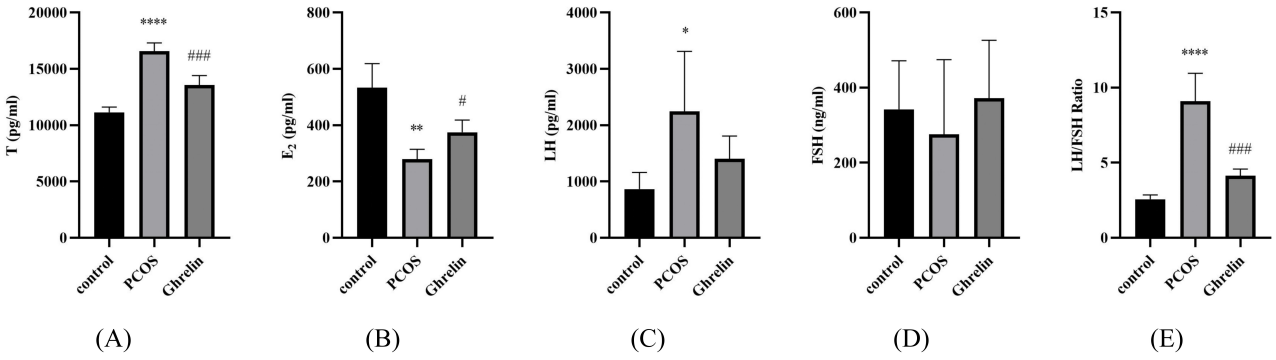

Fig. 9. Ghrelin impacts on sex hormones in PCOS mice (n = 8). Serum sex hormones were detected by ELISA. (A) Testosterone. (B) Estradiol. (C) Luteinizing hormone. (D) Follicle-stimulating hormone. (E) LH/FSH ratio. *, **, and ****: $p < 0.05$, 0.01, and 0.0001 vs. control group; # and ###: $p < 0.05$ and 0.001 vs. PCOS group.

tal effects of LPS-induced damage to the underlying endothelium. Furthermore, Yin *et al.* [36] have shown that ghrelin might inhibit Kupffer cell M1 polarization and mitigate the development of nonalcoholic steatohepatitis caused by continuous low-grade inflammation. Carneiro *et al.* [37] confirmed the inhibitory impact of ghrelin on insulin production in obese Zücker rats.

In our investigation, a KGN cell inflammation model was applied via the administration of LPS. This resulted in an upregulation of mRNA expression and subsequent IL-1β, TNF-α, and IL-6 protein synthesis. The potential mitigation of these consequences might be achieved with the administration of ghrelin. Subsequent experiments revealed that the application of TAK242, a TLR4 inhibitor, prior to exposing KGN cells led to suppressing the inflammation generated by LPS. Furthermore, ghrelin administration has shown an additional capacity to reduce the production of inflammatory markers.

To further confirm the therapeutic impact of ghrelin on PCOS, we employed a high-fat diet and DHEA-generated PCOS mouse model. The findings demonstrate that PCOS models with obesity, IR, and irregular ovulation may be influenced via a high-fat diet and DHEA. When Zhang *et al.* [38] administered 60 mg/kg/d DHEA to mice for three weeks, they created a PCOS model characterized by weight gain, high estrogen levels, hyperandrogen-

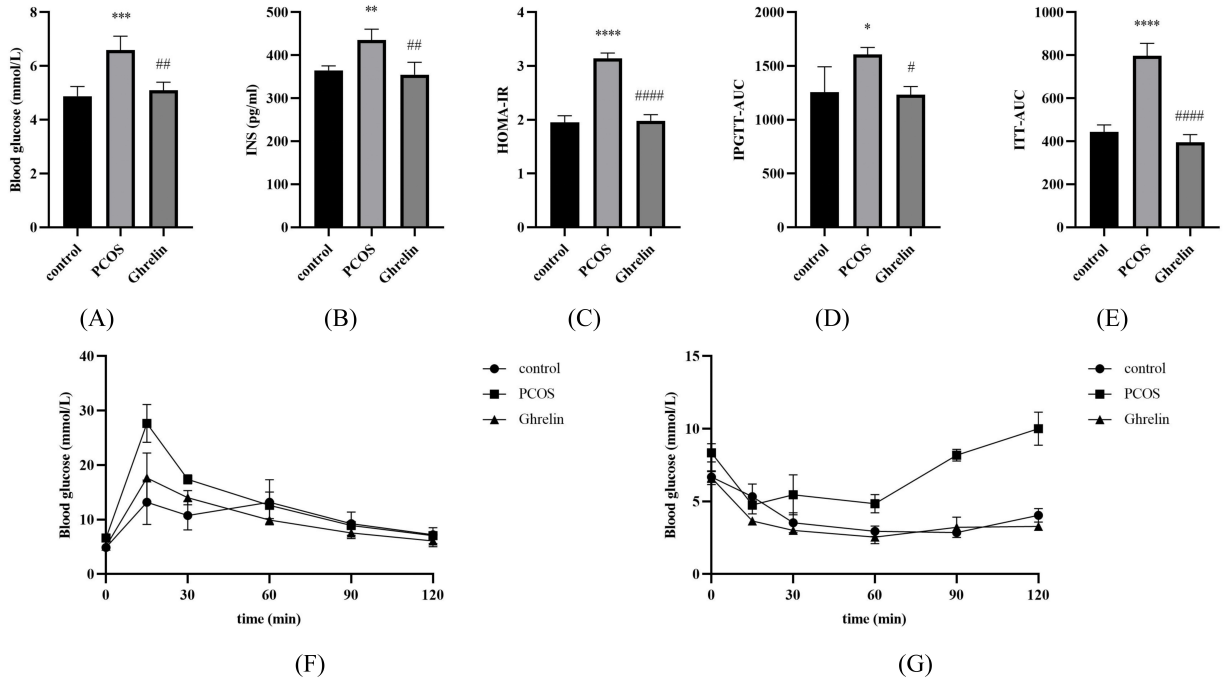

Fig. 10. Ghrelin impacts on PCOS mice-related insulin resistance. (A) Glucose oxidase-based blood glucose measurement in mice following overnight fasting (n = 4). (B) ELISA-based mice serum insulin level following overnight fasting (n = 4). (C) HOMA-IR was estimated after detecting the mice's blood insulin and glucose values (n = 4). (D) IPGTT AUC values (n = 4). (E) ITT AUC values (n = 4). (F) Blood glucose values after intraperitoneal injection of glucose at 0, 15, 30, 60, 90, 120 min (n = 4). (G) Blood glucose values after intraperitoneal injection of insulin at 0, 15, 30, 60, 90, 120 min (n = 4). *, **, *** and ****: $p < 0.05$, 0.01, 0.001, and 0.0001 vs. control group; similarly, $^{\#}$, $^{\#\#}$ and $^{\#\#\#\#}$: $p < 0.05$, 0.01, and 0.0001 vs. PCOS group. IPGTT, intraperitoneal glucose test; AUC, area under the curve; ITT, insulin tolerance test.

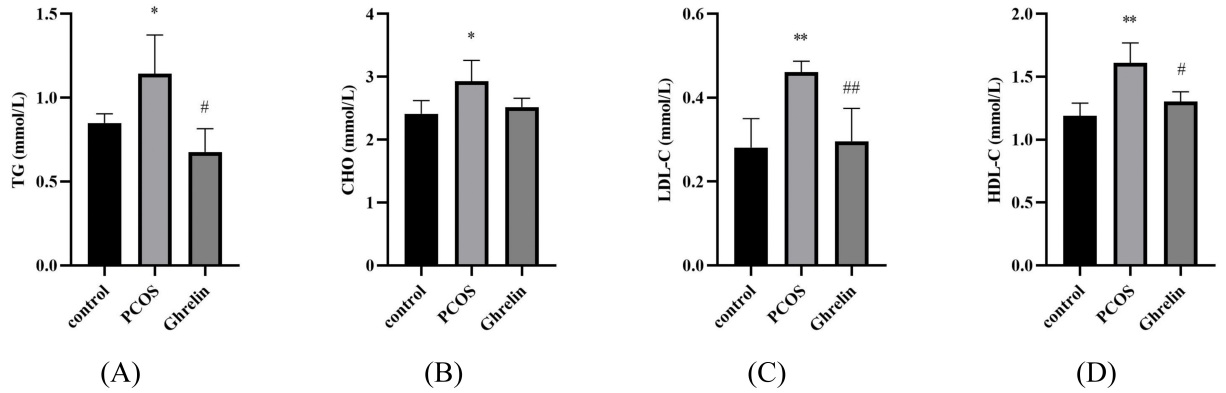

Fig. 11. Ghrelin impacts lipid metabolism in PCOS mice (n = 4). Automatic biochemical analyzer-based measurements of blood lipid metabolism indicators. (A) TG. (B) CHO. (C) LDL-C. (D) HDL-C. * and **: $p < 0.05$ and 0.01 vs. control group; $^{\#}$ and $^{\#\#}$: $p < 0.05$ and 0.01 vs. PCOS group. TG, triglyceride; CHO, cholesterol; LDL-C, low-density lipoprotein cholesterol; HDL-C, high-density lipoprotein cholesterol.

emia, and an elevated LH/FSH ratio. This model also resulted in a disruption of the estrous cycle, which mostly manifested as an estrus cycle distribution. Li *et al.* [39] produced a PCOS-IR model via a high-fat diet and letrozole, which was characterized by hyperinsulinemia, hyperandrogenemia, an increased LH/FSH ratio, and aberrant lipid metabolism (greater CHO, TG, and LDL-C and decreased HDL-C). Our research also showed that PCOS mice had an irregular estrous cycle, increased body fat, hyperandrogenism, and an abnormally high LH/FSH ratio. Es-

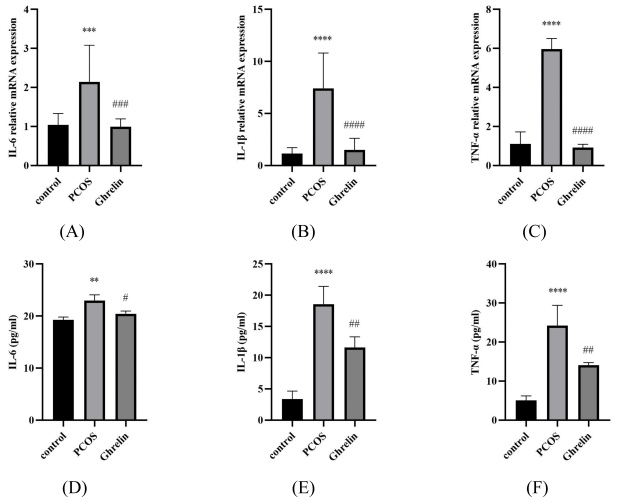

Fig. 12. Ghrelin impacts on inflammation indicators (n = 4). (A) IL-6, (B) IL-1β, and (C) TNF-α, mRNA expression within mice ovarian tissues were detected by RT-qPCR. Serum levels of (D) IL-6, (E) IL-1β, and (F) TNF-α measured by ELISA. **, ***, ****: $p < 0.01$, 0.001, and 0.0001 vs. control group; $^{\#}$, $^{\#\#}$, $^{\#\#\#}$ and $^{\#\#\#\#}$: $p < 0.05$, 0.01, 0.001, and 0.0001 vs. PCOS group.

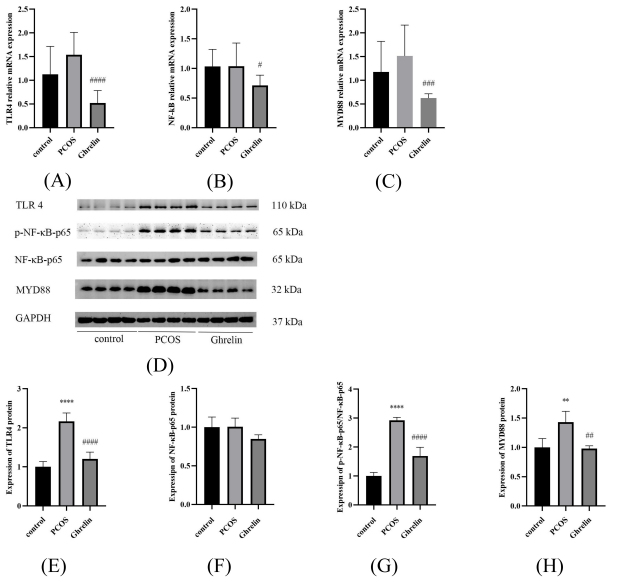

Fig. 13. Ghrelin impacts on the TLR4/NF-κB signaling pathway (n = 4). TLR4, NF-κB, and MYD88 mRNA expression within mice ovarian tissues was measured via RT-qPCR. (A) TLR4. (B) NF-κB. (C) MYD88. (D–H) Western blotting-based measurement of TLR4, p-NF-κB-p65, NF-κB-p65, and MYD88 protein expression. ** and ****: $p < 0.01$ and 0.0001 vs. control group; similarly, $^{\#}$, $^{\#\#}$, $^{\#\#\#}$ and $^{\#\#\#\#}$: $p < 0.05$, 0.01, 0.001 and 0.0001 vs. PCOS group.

trous stagnation was most noticeable during metestrus and diestrus, and estrogen levels were more diminished than among controls. Our model mice similarly had an aberrant lipid metabolism, although their HDL-C levels were better than those of the control animals. Mice in our research still exhibited IR, reproductive abnormalities, and lipid metabolism abnormalities despite our PCOS model being remarkably different from the one utilized by Zhang *et al.* [38] and Li *et al.* [39]. PCOS mice treated with ghrelin for three weeks showed substantial improvements in IR, reproductive abnormalities, lipid metabolic abnormalities, and inflammation. Nonalcoholic fatty liver disease is treated with ghrelin because it reduces insulin resistance, as shown by Gong *et al.* [40]. Tsaban *et al.* [41] found that ghrelin reflected insulin sensitivity. Moreover, treatment with EXT418, a long-acting ghrelin, reduced inflammation in mouse skeletal muscles, as shown by Kerr *et al.* [42]. Our results show that once a PCOS model was established, ghrelin administration substantially reduced serum inflammatory marker expression, INS levels, HOMA-IR indices, IPGTT and ITT AUC values, and mRNA and protein levels of inflammatory component expression within ovarian tissues. Moreover, the estrous cycles of PCOS mice reverted to near-normal levels, and the high LH/FSH ratio and hyperandrogenemia improved. These findings suggest that ghrelin might help treat PCOS by correcting metabolic and reproductive problems associated with insulin resistance, inflammation, and lipid metabolism.

Several diseases and their association with TLR signaling pathways have been established. TLRs are type 1 transmembrane proteins that detect and react to pathogen-associated molecular patterns (PAMPs) [43]. TLR4 may attract MYD88, a signaling molecule, and activate it to trigger the release of cytokines with subsequent NF-κB phosphorylation [44]. There is evidence linking the TLR4 signaling pathway to PCOS pathophysiology. Hu *et al.* [45] found that PCOS patients have greater TLR4 and NF-κB protein concentrations than controls. Ren *et al.* [46] revealed that TLR4 signaling pathway expression was enhanced in PCOS-like rats, indicating that the TLR4 signaling pathway could be implicated in PCOS. TLR4 was also involved in alterations to the gut microbiota of rats with letrozole-induced PCOS, as was discovered by Wang *et al.* [47]. We examined the signaling pathway TLR4/NF-κB within KGN cells and mice ovarian tissues, analyzing protein and mRNA expression parameters. NF-κB, TLR4, and MYD88 expression were increased in KGN cells in response to LPS, whereas ghrelin pretreatment suppressed this effect. Higher NF-κB and TLR4 mRNA levels could be seen within the PCOS model, and their expression was suppressed in response to ghrelin treatment. In addition, ghrelin administration decreased p-NF-κB and TLR4 protein expression. Subsequently, it is evidenced that ghrelin may have a role in PCOS through the TLR4/NF-κB signaling pathway.

Our investigation is the first to explain ghrelin's beneficial impacts on PCOS in animal models and KGN cells. However, our findings are limited to studies conducted in

animal and cell cultures. Further clinical research is required to confirm the causal connection between ghrelin and PCOS.

Conclusions

Ghrelin might ameliorate inflammation, insulin resistance, and reproductive abnormalities in PCOS mice brought on by DHEA and a high-fat diet through the TLR4/NF-κB signaling pathway. Ghrelin is promising as a potential new medication for PCOS. Further research is needed to determine whether other processes contribute to its therapeutic benefits.

Availability of Data and Materials

All data generated or analyzed during this study are included in this article. Further inquiries can be directed to the corresponding author.

Author Contributions

Conceptualization: FL, XW, MZ, KZ, CL, HL and LX. Visualization: FL, KZ, CL. Supervision: LX. Writing original draft preparation, review and editing: FL, XW, MZ, KZ, CL, HL and LX. Funding acquisition: LX. All authors have given final approval of the version to be published. Each author participated sufficiently in the work and agreed to be accountable for all aspects of the work.

Ethics Approval and Consent to Participate

This study protocol was reviewed and approved by the Animal Ethics Review Committee of the Affiliated Hospital of Qingdao University, approval number: AHQU-MAL20230630.

Acknowledgment

Not applicable.

Funding

This research was supported by National Natural Science Foundation of China (81571408).

Conflict of Interest

The authors declare no conflict of interest.

References

[1] He S, Ji D, Liu Y, Deng X, Zou W, Liang D, *et al*. Correction to: Polymorphisms of mtDNA in the D-loop region moderate the associations of BMI with HOMA-IR and HOMA-β among women with polycystic ovary syndrome: a cross-sectional study. Journal of Assisted Reproduction and Genetics. 2023; 40: 2277.

[2] Zheng CY, Yu YX, Bai X. Polycystic ovary syndrome and related inflammation in radiomics; relationship with patient outcome. Seminars in Cell & Developmental Biology. 2024; 154: 328–333.

[3] Al-Awadi AM, Saldhana FL, Bauyrzhanova Z, Nemr R, Mahmood NA, Almawi WY. Relation of resistin gene variants to resistin plasma levels and altered susceptibility to polycystic ovary syndrome: A case control study. American Journal of Reproductive Immunology (New York, N.Y.: 1989). 2023; 90: e13731.

[4] Zeng H, Huang Y, Liu D, Xie T, Chen Z, Huang Q, *et al*. Interaction between OCT1 and LPIN1 polymorphisms and response to pioglitazone-metformin tablets in patients with polycystic ovary syndrome. Chinese Medical Journal. 2023; 136: 1756–1758.

[5] Li J, Chen S, Qin R, Liu X, Fan L, Wei M, *et al*. Talin1 regulates glucose metabolism and endometrial receptivity *via* GLUT-4 in patients with polycystic ovary syndrome and insulin resistance. Gynecological Endocrinology: the Official Journal of the International Society of Gynecological Endocrinology. 2023; 39: 2231085.

[6] Shahmoradi S, Chiti H, Tavakolizadeh M, Hatami R, Motamed N, Ghaemi M. The Effect of Magnesium Supplementation on Insulin Resistance and Metabolic Profiles in Women with Polycystic Ovary Syndrome: a Randomized Clinical Trial. Biological Trace Element Research. 2023. (online ahead of print)

[7] Liang R, Sheng M, Li X, Jin J, Yi Y. Transcriptomic analysis reveals that the anti-PCOS effects of Zishen Qingre Lishi Huayu recipe may involve pathways and genes related to autophagy, steroidogenesis, oxidative stress, and inflammation in granulosa cells. Journal of Ethnopharmacology. 2023; 314: 116551.

[8] Zhang Y, Lin Y, Li G, Yuan Y, Wang X, Li N, *et al*. Glucagon-like peptide-1 receptor agonists decrease hyperinsulinemia and hyperandrogenemia in dehydroepiandrosterone-induced polycystic ovary syndrome mice and are associated with mitigating inflammation and inducing browning of white adipose tissue†. Biology of Reproduction. 2023; 108: 945–959.

[9] Xie Q, Hong W, Li Y, Ling S, Zhou Z, Dai Y, *et al*. Chitosan oligosaccharide improves ovarian granulosa cells inflammation and oxidative stress in patients with polycystic ovary syndrome. Frontiers in Immunology. 2023; 14: 1086232.

[10] Mazloomi S, Barartabar Z, Pilehvari S. The Association Between Increment of Interleukin-1 and Interleukin-6 in Women with Polycystic Ovary Syndrome and Body Mass Index. Journal of Reproduction & Infertility. 2023; 24: 26–34.

[11] Kwok KO, Fries LR, Silva-Zolezzi I, Thakkar SK, Iroz A, Blanchard C. Effects of Probiotic Intervention on Markers of Inflammation and Health Outcomes in Women of Reproductive Age and Their Children. Frontiers in Nutrition. 2022; 9: 889040.

[12] Zhai Y, Pang Y. Systemic and ovarian inflammation in women with polycystic ovary syndrome. Journal of Reproductive Immunology. 2022; 151: 103628.

[13] Vaez S, Parivr K, Amidi F, Rudbari NH, Moini A, Amini N. Quercetin and polycystic ovary syndrome; inflammation, hormonal parameters and pregnancy outcome: A randomized clinical trial. American Journal of Reproductive Immunology (New York, N.Y.: 1989). 2023; 89: e13644.

[14] Lai Y, Ye Z, Mu L, Zhang Y, Long X, Zhang C, *et al*. Elevated Levels of Follicular Fatty Acids Induce Ovarian Inflammation via ERK1/2 and Inflammasome Activation in PCOS. The Journal of Clinical Endocrinology and Metabolism. 2022; 107: 2307–2317.

[15] Deng J, Hu Y, Zhang Y, Yu F. Ghrelin improves endothelial function and reduces blood pressure in Ang II-induced hypertensive mice: Role of AMPK. Clinical and Experimental Hypertension (New York, N.Y.: 1993). 2023; 45: 2208774.

[16] Yurci A, Dokuzeylül Güngör N, Güngör K, Hatırnaz Ş. Correlation of serum leptin and ghrelin levels with endocrine and reproductive parameters in women with clomiphene citrate resistant polycystic ovary syndrome. Turkish Journal of Obstetrics and Gynecology. 2022; 19: 124–129.

[17] Polak AM, Krentowska A, Łebkowska A, Buczyńska A, Adamski M, Adamska-Patruno E, *et al*. The Association of

Serum Levels of Leptin and Ghrelin with the Dietary Fat Content in Non-Obese Women with Polycystic Ovary Syndrome. Nutrients. 2020; 12: 2753.

[18] Stark R, Feehan J, Mousa A, Andrews ZB, de Courten B. Liver-expressed antimicrobial peptide 2 is associated with improved pancreatic insulin secretion in adults with overweight and obesity. Diabetes, Obesity & Metabolism. 2023; 25: 1213–1220.

[19] Yuan PQ, Wu SV, Wang L, Taché Y. The ghrelin agonist, HM01 activates central vagal and enteric cholinergic neurons and reverses gastric inflammatory and ileus responses in rats. Neurogastroenterology and Motility. 2023; 35: e14561.

[20] Li G, Liu J, Xia WF, Zhou CL, Lv LQ. Protective effects of ghrelin in ventilator-induced lung injury in rats. International Immunopharmacology. 2017; 52: 85–91.

[21] Guan HY, Xia HX, Chen XY, Wang L, Tang ZJ, Zhang W. Toll-Like Receptor 4 Inhibits Estradiol Secretion *via* NF-κB Signaling in Human Granulosa Cells. Frontiers in Endocrinology. 2021; 12: 629554.

[22] Wang Y, Yang Q, Wang H, Zhu J, Cong L, Li H, *et al*. NAD+ deficiency and mitochondrial dysfunction in granulosa cells of women with polycystic ovary syndrome‡. Biology of Reproduction. 2021; 105: 371–380.

[23] Kwak SY, Shim S, Park S, Kim H, Lee SJ, Kim MJ, *et al*. Ghrelin reverts intestinal stem cell loss associated with radiation-induced enteropathy by activating Notch signaling. Phytomedicine: International Journal of Phytotherapy and Phytopharmacology. 2021; 81: 153424.

[24] Ezquerro S, Tuero C, Becerril S, Valentí V, Moncada R, Landecho MF, *et al*. Antagonic effect of ghrelin and LEAP-2 on hepatic stellate cell activation and liver fibrosis in obesity-associated nonalcoholic fatty liver disease. European Journal of Endocrinology. 2023; 188: 564–577.

[25] Yakabi K, Ro S, Onouhi T, Tanaka T, Ohno S, Miura S, *et al*. Histamine mediates the stimulatory action of ghrelin on acid secretion in rat stomach. Digestive Diseases and Sciences. 2006; 51: 1313–1321.

[26] Zhang L, Fernando T, Liu Y, Liu Y, Zhu X, Li M, *et al*. Neurokinin 3 receptor antagonist-induced adipocyte activation improves obesity and metabolism in PCOS-like mice. Life Sciences. 2022; 310: 121078.

[27] Luo M, Zheng LW, Wang YS, Huang JC, Yang ZQ, Yue ZP, *et al*. Genistein exhibits therapeutic potential for PCOS mice *via* the ER-Nrf2-Foxo1-ROS pathway. Food & Function. 2021; 12: 8800–8811.

[28] Jeanes YM, Reeves S. Metabolic consequences of obesity and insulin resistance in polycystic ovary syndrome: diagnostic and methodological challenges. Nutrition Research Reviews. 2017; 30: 97–105.

[29] Macut D, Simic T, Lissounov A, Pljesa-Ercegovac M, Bozic I, Djukic T, *et al*. Insulin resistance in non-obese women with polycystic ovary syndrome: relation to byproducts of oxidative stress. Experimental and Clinical Endocrinology & Diabetes. 2011; 119: 451–455.

[30] Zhang N, Liu X, Zhuang L, Liu X, Zhao H, Shan Y, *et al*. Berberine decreases insulin resistance in a PCOS rats by improving GLUT4: Dual regulation of the PI3K/AKT and MAPK pathways. Regulatory Toxicology and Pharmacology: RTP. 2020; 110: 104544.

[31] Arvat E, Maccario M, Di Vito L, Broglio F, Benso A, Gottero C, *et al*. Endocrine activities of ghrelin, a natural growth hormone secretagogue (GHS), in humans: comparison and interactions with hexarelin, a nonnatural peptidyl GHS, and GH-releasing hormone. The Journal of Clinical Endocrinology and Metabolism. 2001; 86: 1169–1174.

[32] Lin Y, Matsumura K, Fukuhara M, Kagiyama S, Fujii K, Iida M. Ghrelin acts at the nucleus of the solitary tract to decrease arterial pressure in rats. Hypertension (Dallas, Tex.: 1979). 2004; 43: 977–982.

[33] Liu XY, Wei DG, Li RS. Ghrelin attenuates inflammation in diabetic lung disease by TLR4 pathway in vivo and in vitro. BMJ Open Diabetes Research & Care. 2023; 11: e003027.

[34] Bai J, Jiang G, Zhao M, Wang S. Ghrelin Mitigates High-Glucose-Induced Oxidative Damage and Apoptosis in Lens Epithelial Cells. Journal of Diabetes Research. 2022; 2022: 1373533.

[35] Ge S, He W, Zhang L, Lin S, Luo Y, Chen Q, *et al*. Ghrelin pretreatment enhanced the protective effect of bone marrow-derived mesenchymal stem cell-conditioned medium on lipopolysaccharide-induced endothelial cell injury. Molecular and Cellular Endocrinology. 2022; 548: 111612.

[36] Yin Y, Wang Q, Qi M, Zhang C, Li Z, Zhang W. Ghrelin ameliorates nonalcoholic steatohepatitis induced by chronic low-grade inflammation via blockade of Kupffer cell M1 polarization. Journal of Cellular Physiology. 2021; 236: 5121–5133.

[37] Carneiro L, Fenech C, Liénard F, Grall S, Abed B, Haydar J, *et al*. Hypothalamic Glucose Hypersensitivity-Induced Insulin Secretion in the Obese Zücker Rat Is Reversed by Central Ghrelin Treatment. Antioxidants & Redox Signaling. 2023. (online ahead of print.)

[38] Zhang H, Zheng L, Li C, Jing J, Li Z, Sun S, *et al*. Effects of gut microbiota on omega-3-mediated ovary and metabolic benefits in polycystic ovary syndrome mice. Journal of Ovarian Research. 2023; 16: 138.

[39] Li M, Gao S, Kang M, Zhang X, Lan P, Wu X, *et al*. Quercitrin alleviates lipid metabolism disorder in polycystic ovary syndrome-insulin resistance by upregulating PM20D1 in the PI3K/Akt pathway. Phytomedicine: International Journal of Phytotherapy and Phytopharmacology. 2023; 117: 154908.

[40] Gong Y, Guo Y, Jiang Y, Xing Z, Zhang H, Wang H, *et al*. Intracerebroventricular injection of ghrelin receptor antagonist alleviated NAFLD via improving hypothalamic insulin resistance. Iranian Journal of Basic Medical Sciences. 2022; 25: 1117–1122.

[41] Tsaban G, Yaskolka Meir A, Zelicha H, Rinott E, Kaplan A, Shalev A, *et al*. Diet-induced Fasting Ghrelin Elevation Reflects the Recovery of Insulin Sensitivity and Visceral Adiposity Regression. The Journal of Clinical Endocrinology and Metabolism. 2022; 107: 336–345.

[42] Kerr HL, Krumm K, Lee IIG, Anderson B, Christiani A, Strait L, *et al*. EXT418, a novel long-acting ghrelin, mitigates Lewis lung carcinoma induced cachexia in mice. Journal of Cachexia, Sarcopenia and Muscle. 2023; 14: 1337–1348.

[43] Akira S, Takeda K. Toll-like receptor signalling. Nature Reviews. Immunology. 2004; 4: 499–511.

[44] Chen L, Zheng L, Chen P, Liang G. Myeloid Differentiation Primary Response Protein 88 (MyD88): The Central Hub of TLR/IL-1R Signaling. Journal of Medicinal Chemistry. 2020; 63: 13316–13329.

[45] Hu M, Zhang Y, Li X, Cui P, Sferruzzi-Perri AN, Brännström M, *et al*. TLR4-Associated IRF-7 and NFκB Signaling Act as a Molecular Link Between Androgen and Metformin Activities and Cytokine Synthesis in the PCOS Endometrium. The Journal of Clinical Endocrinology and Metabolism. 2021; 106: 1022–1040.

[46] Ren Y, Ye Y, Xuan F, Chen A, Jin R, Zhou W, *et al*. The effect of sitagliptin combined with rosiglitazone on autophagy and inflammation in polycystic ovary syndrome by regulating PI3K/AKT/mTOR and TLR4/NF-κB pathway. Reproductive Biology. 2023; 23: 100763.

[47] Wang Y, Xiao H, Liu Y, Tong Q, Yu Y, Qi B, *et al*. Effects of Bu Shen Hua Zhuo formula on the LPS/TLR4 pathway and gut microbiota in rats with letrozole-induced polycystic ovary syndrome. Frontiers in Endocrinology. 2022; 13: 891297.